THE JOURNAL OF PHYSICAL CHEMISTRY C

Article

Cite This: J. Phys. Chem. C 2019, 123, 30467−30472

pubs.acs.org/JPCC

On-Surface Intramolecular Dehalogenation of Vicinal Dibromides for the Direct Formation of C−C Double Bonds

Xin Yu,[†] Haiping Lin,[‡] Yingke Yang,[‡] Liangliang Cai,[†] and Wei Xu*,[†]

[†]Interdisciplinary Materials Research Center, College of Materials Science and Engineering, Tongji University, Shanghai 201804, P. R. China

[‡]Institute of Functional Nano & Soft Materials (FUNSOM), Jiangsu Key Laboratory for Carbon-Based Functional Materials & Devices, Joint International Research Laboratory of Carbon-Based Functional Materials and Devices, Soochow University, Suzhou, 215123 Jiangsu, P. R. China

Supporting Information

ABSTRACT: The intramolecular dehalogenation reaction as an essential step is generally involved in the deprotection of carbon−carbon double bonds in solution chemistry. However, harsh reaction conditions often limit the functional group compatibility and cause the selectivity problems. In comparison with traditional solution reactions, on-surface chemical reactions always occur on metal substrates, which could serve as catalysts to effectively reduce the reaction barriers in many cases. On the other hand, on-surface intermolecular dehalogenative homocoupling reactions have been extensively demonstrated, while, to our knowledge, intramolecular dehalogenation reactions are less discussed on surfaces. Herein, by the combination of high-resolution scanning tunneling microscopy imaging and density functional theory calculations, we introduce the vicinal dibromo group on chemically different surfaces, such as Cu(110), Ag(110), and Au(111), respectively, to investigate the generality of intramolecular dehalogenation reactions. As a result, we successfully achieved the direct formation of C−C double-bonded products in a facile manner on all three surfaces.

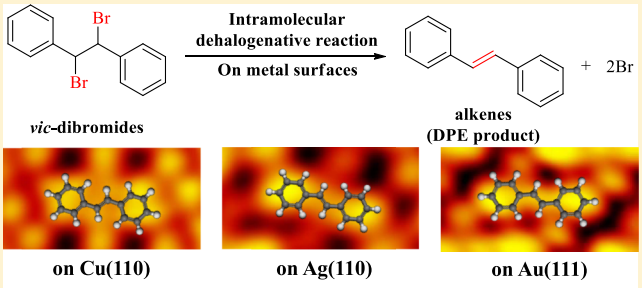

INTRODUCTION

In solution chemistry, vicinal dihalogenation and subsequent dehalogenation have been employed as a normal method for the protection of C−C double bonds in a multistep synthesis process.[1] The corresponding dehalogenation process, however, is very challenging, which often requires highly toxic metal reductants, such as zinc, iron, or metal hydrides.[2,3] To overcome the problem, as a relatively mild condition, varied photosensitizers and photocatalysts have been developed to promote the absorption of visible light for the dehalogenation.[4,5] However, organic additives are still inevitable.[6] In comparison with solution chemistry, on-surface synthesis has attracted a lot of attention in recent years, in which atomically precise fabrication of various structural motifs including C−C double-bonded and triple-bonded nanostructures has been achieved in a facile way.[7−10] Since last dozen years, various chemical reactions have been introduced on surfaces.[11−22] Among others, intermolecular dehalogenative homocoupling reactions have been widely studied and employed to achieve on-surface fabrication of a variety of nanostructures with atomic precision.[23−25] Most intermolecular dehalogenative homocouplings resulted in the formation of C−C single bonds.[26−31] Recently, by introduction of halide precursors containing two and three halogens attached to a carbon atom, our group achieved the direct formation of C−C double-bonded (cf. Scheme 1, upper panel) and triple-bonded structural motifs through intermolecular dehalogenative homocouplings.[7−9] On the other hand, intramolecular dehydrogenation reactions resulting in the formation of C−C

Scheme 1. Illustration Shows the Intermolecular Dehaolegenative Homocoupling of *gem*-Dibromides and the Intramolecular Dehalogenation of *vic*-Dibromides for the Direct Formation of C−C Double-Bonded Structural Motifs

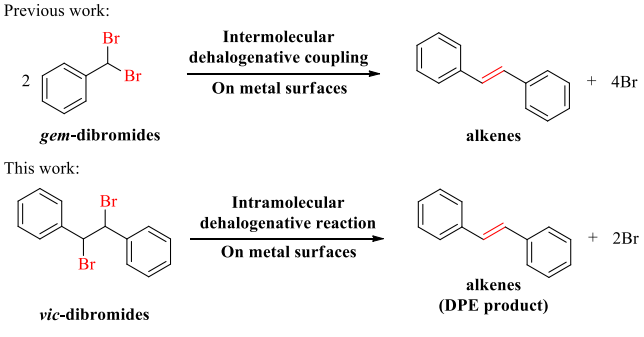

Received: October 15, 2019
Revised: November 20, 2019
Published: November 25, 2019

DOI: 10.1021/acs.jpcc.9b09713
J. Phys. Chem. C 2019, 123, 30467−30472

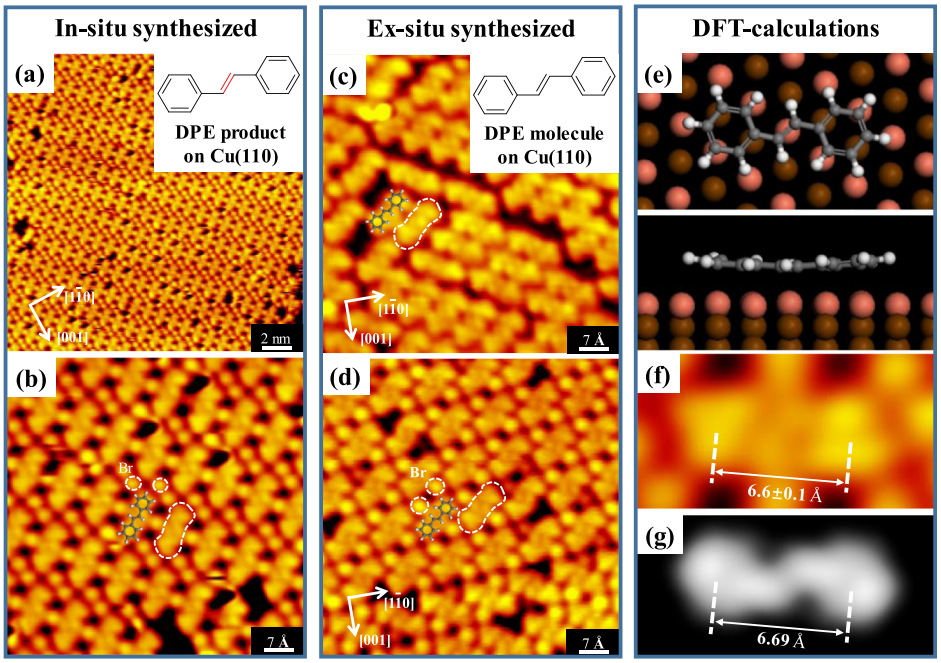

Figure 1. (a) Large-scale and (b) close-up STM images showing the in situ-synthesized DPE products via the intramolecular dehalogenation of *vic*-dibromides on Cu(110). (c,d) STM image of ex situ-synthesized DPE molecules on Cu(110) without and with Br atoms, respectively. The equally scaled model of the DPE molecule is overlaid on the corresponding STM topography, and the in situ-formed DPE product and the ex situ DPE molecules are indicated by white contours as shown in (b,c,d), respectively. The detached Br atoms are indicated by circles in (b,d). (e) Top and side views of the DFT-optimized model of the DPE molecule on Cu(110). (f) High-resolution STM image of the DPE molecule and (g) corresponding simulated STM image with the measured dimensions.

single bonds have been reported.[32−34] However, to our knowledge, the direct formation of C−C double bonds via intramolecular dehalogenation reactions are less discussed on surfaces.[35] Thus, it is of general interest to extend on-surface strategies by investigation of intramolecular dehalogenation reactions.

To explore the intramolecular dehalogenative reactions, in this work, we introduce vicinal (*vic*-) dibromides on metal surfaces. As such, we choose a simple molecule (1,2-dibromo-1,2-diphenylethane, shortened as DBDPE), which has a *vic*-dibromo group in the middle of the two benzene rings as shown in Scheme 1 lower panel. Three chemically different metal substrates, Cu(110), Ag(110), and Au(111), are employed as both templates and catalysts to adopt molecules and to facilitate the on-surface intramolecular dehalogenative reactions. From the interplay of high-resolution scanning tunneling microscopy (STM) imaging and density functional theory (DFT) calculations, we demonstrate that it is feasible to induce intramolecular dehalogenative reactions in a facile manner on surfaces, and as a result, we successfully achieved the direct formation of the C−C double-bonded product, that is, the alkene molecule (1,2-diphenylethene, shortened as DPE) (also see Scheme 1, lower panel). In addition, the in situ-formed product has also been proved by the ex situ-synthesized DPE molecule.

METHODS

The STM experiments were carried out in a UHV chamber with a base pressure of 1×10^{-10} mbar. The whole system is equipped with a variable-temperature "Aarhus-type" scanning tunneling microscope,[36,37] a molecular evaporator, and standard facilities for sample preparation. The metal substrates were prepared by several cycles of 1.5 keV Ar^+ sputtering followed by annealing, resulting in clean and flat terraces separated by monatomic steps. After the system was thoroughly degassed, the DBDPE (from Acros, purity > 97%) and DPE (from TCI, purity > 98%) molecules were sublimated at 300 K. The sample was thereafter transferred within the UHV chamber to the microscope, where measurements were carried out in a typical temperature range of 100−150 K.

The calculations were performed in the framework of DFT by using the Vienna ab initio simulation package (VASP).[38,39] The projector-augmented wave method was used to describe the interaction between ions and electrons,[40,41] and the Perdew−Burke−Ernzerhof (PBE)-generalized gradient approximation exchange−correlation functional was employed.[42] van der Waals corrections to the PBE density functional were also included using the DFT-D3 method of Grimme.[43] The atomic structures were relaxed using the conjugate gradient algorithm scheme as implemented in the VASP code until the forces on all unconstrained atoms were ≤0.03 eV/Å. The simulated STM images were obtained by the Hive program based on the Tersoff−Hamann method.[44]

RESULTS AND DISCUSSION

After deposition of DBDPE molecules on the Cu(110) surface held at room temperature (RT), we observe the formation of ordered islands as shown in Figure 1a,b. From the corresponding close-up STM image (Figure 1b), we identify that the formed molecular islands are composed of rodlike structures and bright protrusions. The rodlike structure is imaged as two lobes at both ends linked by two dot-shaped contrasts in the center. According to the previous studies,[7−9,21,29] the round bright spots are attributed to detached bromine atoms. We thus speculate that the intramolecular dehalogenative reactions have occurred. Because of the

DOI: 10.1021/acs.jpcc.9b09713
J. Phys. Chem. C 2019, 123, 30467−30472

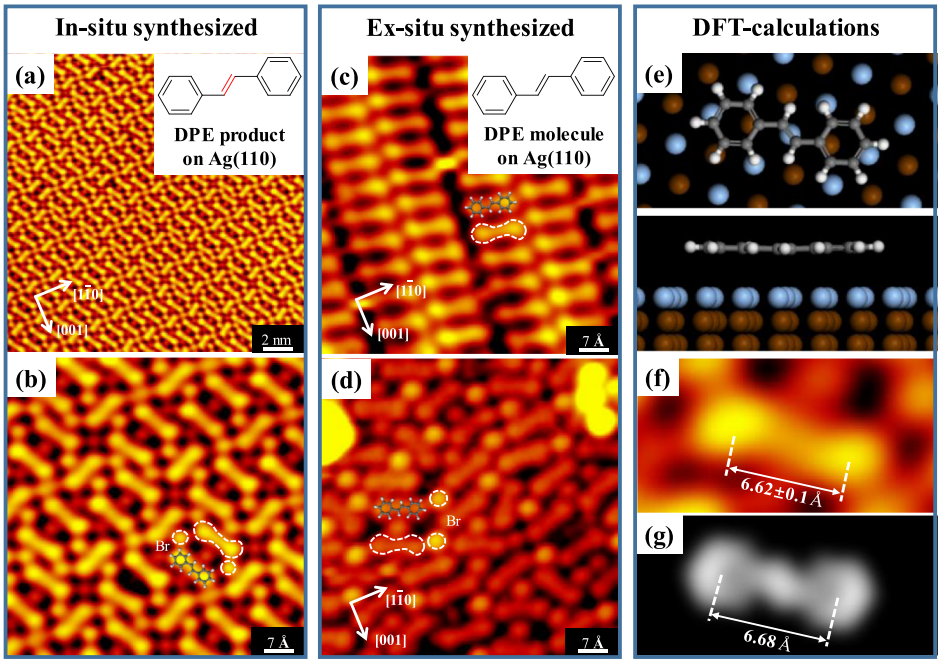

Figure 2. (a) Large-scale and (b) close-up STM images showing the in situ-synthesized DPE products via the intramolecular dehalogenation of *vic*-dibromides on Ag(110). (c,d) STM images of ex situ-synthesized DPE molecules on Ag(110) without and with Br atoms, respectively. (e) Top and side views of the DFT-optimized model of the DPE molecule on Ag(110). (f) High-resolution STM image of the DPE molecule and (g) corresponding simulated STM image with the measured dimensions.

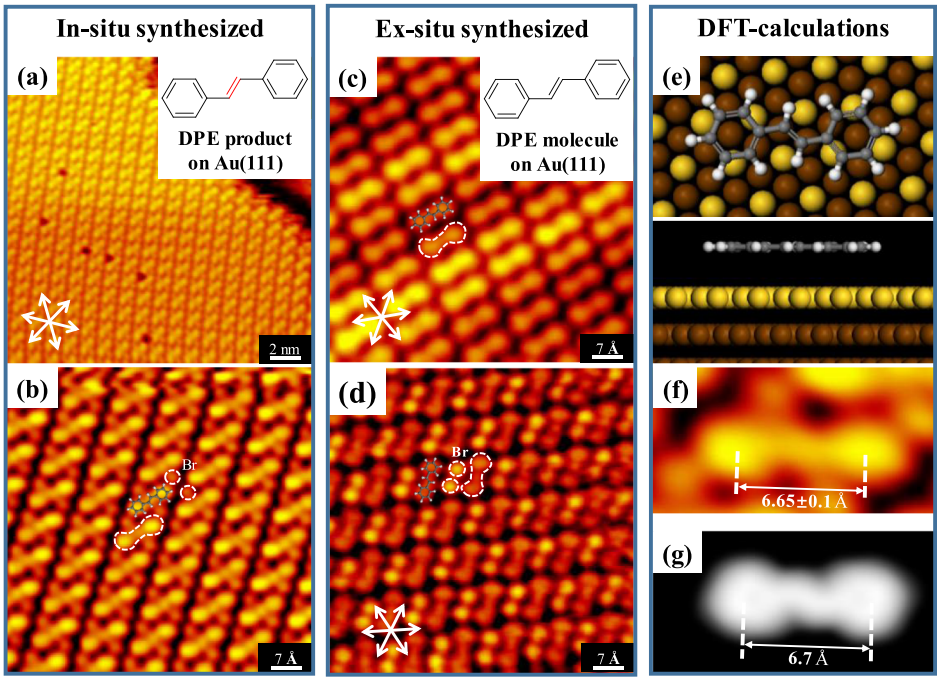

Figure 3. (a) Large-scale and (b) close-up STM images showing the in situ-synthesized DPE products via the intramolecular dehalogenation of *vic*-dibromides on Au(111). (c,d) STM images of ex situ-synthesized DPE molecules on Au(111) without and with Br atoms, respectively. (e) Top and side views of the DFT-optimized model of the DPE molecule on Au(111). (f) High-resolution STM image of the DPE molecule and (g) corresponding simulated STM image with the measured dimensions.

formation of well-ordered self-assembled islands (Figure 1a), which indicates that the formed rodlike motifs are highly mobile on the surface, we thus further deduce that the rodlike motifs should be attributed to the alkene products, that is, the DPE molecules. To experimentally confirm the in situ formation of DPE molecules, we directly deposit commercialized DPE molecules on the surface, as shown in Figure 1c. As can be seen from the STM image of ex situ-synthesized DPE molecule on Cu(110), we identify that the morphology of the DPE molecule is in good agreement with the in situ-synthesized product. In addition, in order to provide a similar chemical environment, we utilize the residual Br atoms within

DOI: 10.1021/acs.jpcc.9b09713
J. Phys. Chem. C 2019, 123, 30467−30472

the chamber to make Br-participated self-assembled DPE islands as shown in Figure 1d. Again, the STM morphology of the DPE molecule shown in Figure 1d is characteristically the same as the one in Figure 1b. Theoretically, we relax the DPE molecule on Cu(110) as shown in Figure 1e, and based on that, the simulated STM image of the DPE molecule is studied as shown in Figure 1g. From the comparison of the simulated STM image and the close-up STM image of in situ-formed DPE product, both the morphology and the dimension fit well. Based on the above analysis, we draw the conclusion that the intramolecular dehalogenative reaction proceeds on the Cu(110) surface, and as a result, the direct formation of C−C double-bonded alkene product is achieved.

To explore the generality of such an intramolecular dehalogenative reactions and the influence of different metal substrates, we have also performed experiments on Ag(110) as shown in Figure 2a,b. Interestingly, similar to the case on Cu(110), intramolecular debromination of DBDPE also occurs on Ag(110) at RT. A good agreement is also achieved by comparing the ex situ-synthesized DPE molecule and the in situ product, as shown in Figure 2c. The STM morphology of ex situ-synthesized DPE molecule with Br atoms shown in Figure 2d is characteristically the same as the in situ product shown in Figure 2b. Based on the relaxed model (Figure 2e), we perform STM simulations as shown in Figure 2g. From the comparison of the simulated STM image and the close-up STM image of the in situ product, a good agreement is also achieved, which demonstrates that the intramolecular dehalogenative reaction can also proceed on the Ag(110) surface.

In the next step, we move to a chemically even less reactive surface Au(111). As shown in Figure 3a,b, unexpectedly, intramolecular debromination of DBDPE also occurs right after deposition on Au(111) at RT. Both STM results of the ex situ-synthesized DPE molecule (Figure 3c,d) and DFT calculations (Figure 3e,g) fit quite well with the in situ-synthesized product (Figure 3f). More surprisingly, such an intramolecular debrominative reaction could occur at even ∼150 K, indicating that the energy barrier is quite low in comparison with Ullmann reaction ($C(sp^2)$−Br) on the same surface;[14] on the other hand, such an intramolecular debromination is in analogy with Wurtz reaction ($C(sp^3)$−Br).[26]

To further confirm the experimentally observed relatively low temperature of debromination on Au(111), we have performed DFT calculations on the reaction pathway of intramolecular dehalogenation of vicinal dibromides on the Au(111) surface. As shown in Figure 4, the barriers for the successive debromination processes on Au(111) are determined to be 0.15 eV (i.e., ∼56 K according to the Arrhenius equation) for the first Br and 0.40 eV (i.e., ∼150 K) for the second one, respectively, which is in excellent agreement with our experimental conditions and observations. In addition, to confirm that the molecules are intact during deposition, we have performed additional DFT calculations on the reaction pathway of intramolecular dehalogenation of vicinal dibromides in the gas phase. As shown in the Supporting Information, the energy barrier for the debromination process (simultaneous debromination of two Br atoms) in vacuum is determined to be 1.4 eV (i.e., ∼525 K), while, on the other hand, the molecules were experimentally sublimated at 300 K. Thus, we confirm that the molecules should be intact during sublimation.

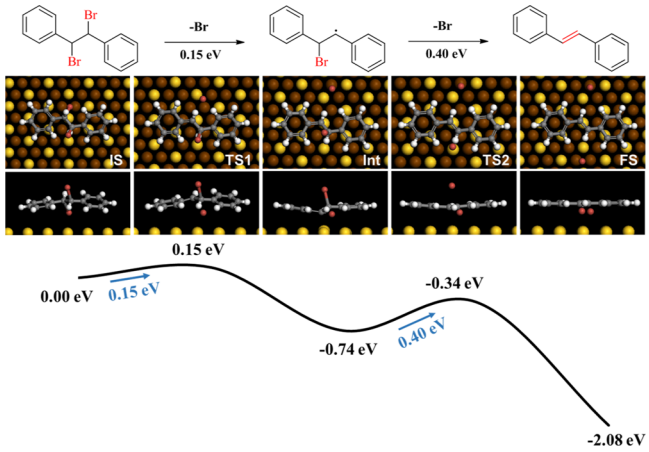

Figure 4. DFT-calculated reaction pathway for the successive C−Br bond activations of the *vic*-dibromide molecule on Au(111). The structural models of the initial state (IS), transition state (TS), intermediate (Int), and final state (FS) along the pathway are also shown.

CONCLUSIONS

In conclusion, from the high-resolution UHV-STM imaging and the DFT calculations, we demonstrate that the direct formation of C−C double-bonded products via intramolecular dehalogenative reaction has been successfully achieved on three chemically different metal substrates, that is, Cu(110), Ag(110), and Au(111), in a facile and efficient manner. It is supposed that this intramolecular reaction is a two-step process. First, the *vic*-diradical intermediate is formed by C−Br bond activation, and second, the intramolecular C−C double bond is spontaneously formed via rearrangement of the diradicals. The findings provide an alternative route for incorporating C−C double bonds into surface nanostructures.

ASSOCIATED CONTENT

Supporting Information

The Supporting Information is available free of charge at https://pubs.acs.org/doi/10.1021/acs.jpcc.9b09713.

DFT-calculated reaction pathway for the C−Br bond activations of the DBDPE molecule in vacuum (PDF)

AUTHOR INFORMATION

Corresponding Author

*E-mail: xuwei@tongji.edu.cn.

ORCID

Haiping Lin: 0000-0002-9948-7060

Wei Xu: 0000-0003-0216-794X

Notes

The authors declare no competing financial interest.

ACKNOWLEDGMENTS

The authors acknowledge the financial support from the National Natural Science Foundation of China (21622307 and 21790351), the Fundamental Research Funds for the Central Universities.

REFERENCES

(1) Wuts, P. G. M.; Greene, T. W. *Greene's Protective Groups on Organic Synthesis*, 4th ed.; John Wiley & Sons: Hoboken, 2007.

DOI: 10.1021/acs.jpcc.9b09713
J. Phys. Chem. C 2019, 123, 30467−30472

(2) Taleshi, M. S.; Seidler-Egdal, R. K.; Jensen, K. B.; Schwerdtle, T.; Francesconi, K. A. Synthesis and Characterization of Arsenolipids: Naturally Occurring Arsenic Compounds in Fish and Algae. *Organometallics* **2014**, *33*, 1397−1403.
(3) Kuivila, H. G.; Menapace, L. W. Reduction of Alkyl Halides by Organotin Hydrides. *J. Org. Chem.* **1963**, *28*, 2165−2167.
(4) Maji, T.; Karmakar, A.; Reiser, O. Visible-Light Photoredox Catalysis: Dehalogenation of Vicinal Dibromo-, α-Halo-, and α,α-Dibromocarbonyl Compounds. *J. Org. Chem.* **2011**, *76*, 736−739.
(5) Goren, Z.; Willner, I. Photochemical and chemical reduction of vicinal dibromides via phase transfer of 4,4'-bipyridinium radical: the role of radical disproportionation. *J. Am. Chem. Soc.* **1983**, *105*, 7764−7765.
(6) McTiernan, C. D.; Pitre, S. P.; Scaiano, J. C. Photocatalytic Dehalogenation of Vicinal Dibromo Compounds Utilizing Sexithiophene and Visible-Light Irradiation. *ACS Catal.* **2014**, *4*, 4034−4039.
(7) Sun, Q.; Tran, B. V.; Cai, L.; Ma, H.; Yu, X.; Yuan, C.; Stöhr, M.; Xu, W. On-Surface Formation of Cumulene by Dehalogenative Homocoupling of Alkenyl gem -Dibromides. *Angew. Chem., Int. Ed.* **2017**, *56*, 12165−12169.
(8) Sun, Q.; Yu, X.; Bao, M.; Liu, M.; Pan, J.; Zha, Z.; Cai, L.; Ma, H.; Yuan, C.; Qiu, X.; Xu, W. Direct Formation of C−C Triple-Bonded Structural Motifs by On-Surface Dehalogenative Homocouplings of Tribromomethyl-Substituted Arenes. *Angew. Chem., Int. Ed.* **2018**, *57*, 4035−4038.
(9) Cai, L.; Yu, X.; Liu, M.; Sun, Q.; Bao, M.; Zha, Z.; Pan, J.; Ma, H.; Ju, H.; Hu, S.; Xu, L.; Zou, J.; Yuan, C.; Jacob, T.; Björk, J.; Zhu, J.; Qiu, X.; Xu, W. Direct Formation of C-C Double-Bonded Structural Motifs by On-Surface Dehalogenative Homocoupling of *gem*-Dibromomethyl Molecules. *ACS Nano* **2018**, *12*, 7959−7966.
(10) Sánchez-Grande, A.; de la Torre, B.; Santos, J.; Cirera, B.; Lauwaet, K.; Chutora, T.; Edalatmanesh, S.; Mutombo, P.; Rosen, J.; Zbořil, R.; Miranda, R.; Björk, J.; Jelínek, P.; Martín, N.; Écija, D. On-Surface Synthesis of Ethynylene-Bridged Anthracene Polymers. *Angew. Chem., Int. Ed.* **2019**, *58*, 6559−6563.
(11) Sun, Q.; Zhang, R.; Qiu, J.; Liu, R.; Xu, W. On-Surface Synthesis of Carbon Nanostructures. *Adv. Mater.* **2018**, *30*, 1705630.
(12) Held, P. A.; Fuchs, H.; Studer, A. Covalent-Bond Formation via On-Surface Chemistry. *Chem.—Eur. J.* **2017**, *23*, 5874−5892.
(13) Li, X.; Zhang, H.; Chi, L. On-Surface Synthesis of Graphyne-Based Nanostructures. *Adv. Mater.* **2019**, *31*, 1804087.
(14) Grill, L.; Dyer, M.; Lafferentz, L.; Persson, M.; Peters, M. V.; Hecht, S. Nano-architectures by Covalent Assembly of Molecular Building Blocks. *Nat. Nanotechnol.* **2007**, *2*, 687−691.
(15) Zhang, Y.-Q.; Kepčija, N.; Kleinschrodt, M.; Diller, K.; Fischer, S.; Papageorgiou, A. C.; Allegretti, F.; Björk, J.; Klyatskaya, S.; Klappenberger, F.; Ruben, M.; Barth, J. V. Homo-Coupling of Terminal Alkynes on a Noble Metal Surface. *Nat. Commun.* **2012**, *3*, 1286.
(16) Gao, H.-Y.; Wagner, H.; Zhong, D.; Franke, J.-H.; Studer, A.; Fuchs, H. Glaser Coupling at Metal Surfaces. *Angew. Chem., Int. Ed.* **2013**, *52*, 4024−4028.
(17) Sun, Q.; Zhang, C.; Li, Z.; Kong, H.; Tan, Q.; Hu, A.; Xu, W. On-Surface Formation of One-Dimensional Polyphenylene through Bergman Cyclization. *J. Am. Chem. Soc.* **2013**, *135*, 8448−8451.
(18) Zhou, H.; Liu, J.; Du, S.; Zhang, L.; Li, G.; Zhang, Y.; Tang, B. Z.; Gao, H.-J. Direct Visualization of Surface-Assisted Two-Dimensional Diyne Polycyclotrimerization. *J. Am. Chem. Soc.* **2014**, *136*, 5567−5570.
(19) Krüger, J.; Pavliček, N.; Alonso, J. M.; Pérez, D.; Guitián, E.; Lehmann, T.; Cuniberti, G.; Gourdon, A.; Meyer, G.; Gross, L.; Moresco, F.; Peña, D. Tetracene Formation by On-Surface Reduction. *ACS Nano* **2016**, *10*, 4538−4542.
(20) Sun, Q.; Cai, L.; Wang, S.; Widmer, R.; Ju, H.; Zhu, J.; Li, L.; He, Y.; Ruffieux, P.; Fasel, R.; Xu, W. Bottom-Up Synthesis of Metalated Carbyne. *J. Am. Chem. Soc.* **2016**, *138*, 1106−1109.
(21) Wang, T.; Lv, H.; Fan, Q.; Feng, L.; Wu, X.; Zhu, J. Highly Selective Synthesis of cis -Enediynes on a Ag(111) Surface. *Angew. Chem., Int. Ed.* **2017**, *56*, 4762−4766.
(22) Gong, Z.; Yang, B.; Lin, H.; Tang, Y.; Tang, Z.; Zhang, J.; Zhang, H.; Li, Y.; Xie, Y.; Li, Q.; Chi, L. Structural Variation in Surface-Supported Synthesis by Adjusting the Stoichiometric Ratio of the Reactants. *ACS Nano* **2016**, *10*, 4228−4235.
(23) Cai, J.; Ruffieux, P.; Jaafar, R.; Bieri, M.; Braun, T.; Blankenburg, S.; Muoth, M.; Seitsonen, A. P.; Saleh, M.; Feng, X.; Müllen, K.; Fasel, R. Atomically Precise Bottom-up Fabrication of Graphene Nanoribbons. *Nature* **2010**, *466*, 470−473.
(24) Ruffieux, P.; Wang, S.; Yang, B.; Sánchez-Sánchez, C.; Liu, J.; Dienel, T.; Talirz, L.; Shinde, P.; Pignedoli, C. A.; Passerone, D.; Dumslaff, T.; Feng, X.; Müllen, K.; Fasel, R. On-surface Synthesis of Graphene Nanoribbons with Zigzag Edge Topology. *Nature* **2016**, *531*, 489−492.
(25) Moreno, C.; Vilas-Varela, M.; Kretz, B.; Garcia-Lekue, A.; Costache, M. V.; Paradinas, M.; Panighel, M.; Ceballos, G.; Valenzuela, S. O.; Peña, D.; Mugarza, A. Bottom-up Synthesis of Multifunctional Nanoporous Graphene. *Science* **2018**, *360*, 199−203.
(26) Sun, Q.; Cai, L.; Ding, Y.; Ma, H.; Yuan, C.; Xu, W. Single-molecule Insight into Wurtz Reactions on Metal Surfaces. *Phys. Chem. Chem. Phys.* **2016**, *18*, 2730−2735.
(27) Sun, Q.; Cai, L.; Ma, H.; Yuan, C.; Xu, W. The Stereoselective Synthesis of Dienes through Dehalogenative Homocoupling of Terminal Alkenyl Bromides on Cu(110). *Chem. Commun.* **2016**, *52*, 6009−6012.
(28) Sun, Q.; Cai, L.; Ma, H.; Yuan, C.; Xu, W. Dehalogenative Homocoupling of Terminal Alkynyl Bromides on Au(111): Incorporation of Acetylenic Scaffolding into Surface Nanostructures. *ACS Nano* **2016**, *10*, 7023−7030.
(29) Eichhorn, J.; Nieckarz, D.; Ochs, O.; Samanta, D.; Schmittel, M.; Szabelski, P. J.; Lackinger, M. On-Surface Ullmann Coupling: The Influence of Kinetic Reaction Parameters on the Morphology and Quality of Covalent Networks. *ACS Nano* **2014**, *8*, 7880−7889.
(30) Chen, Q.; Cramer, J. R.; Liu, J.; Jin, X.; Liao, P.; Shao, X.; Gothelf, K. V.; Wu, K. Steering On-Surface Reactions by a Self-Assembly Approach. *Angew. Chem., Int. Ed.* **2017**, *56*, 5026−5030.
(31) Fan, Q.; Wang, C.; Han, Y.; Zhu, J.; Hieringer, W.; Kuttner, J.; Hilt, G.; Gottfried, J. M. Surface-Assisted Organic Synthesis of Hyperbenzene Nanotroughs. *Angew. Chem., Int. Ed.* **2013**, *52*, 4668−4672.
(32) Ammon, M.; Sander, T.; Maier, S. On-Surface Synthesis of Porous Carbon Nanoribbons from Polymer Chains. *J. Am. Chem. Soc.* **2017**, *139*, 12976−12984.
(33) Rogers, C.; Chen, C.; Pedramrazi, Z.; Omrani, A. A.; Tsai, H.-Z.; Jung, H. S.; Lin, S.; Crommie, M. F.; Fischer, F. R. Closing the Nanographene Gap: Surface-Assisted Synthesis of Peripentacene from 6,6′-Bipentacene Precursors. *Angew. Chem., Int. Ed.* **2015**, *54*, 15143−15146.
(34) Zuzak, R.; Castro-Esteban, J.; Brandimarte, P.; Engelund, M.; Cobas, A.; Piątkowski, P.; Kolmer, M.; Pérez, D.; Guitián, E.; Szymonski, M.; Sánchez-Portal, D.; Godlewski, S.; Peña, D. Building a 22-Ring Nanographene by Combining In-solution and On-surface Syntheses. *Chem. Commun.* **2018**, *54*, 10256−10259.
(35) Pavliček, N.; Schuler, B.; Collazos, S.; Moll, N.; Pérez, D.; Guitián, E.; Meyer, G.; Peña, D.; Gross, L. On-surface Generation and Imaging of Arynes by Atomic Force Microscopy. *Nat. Chem.* **2015**, *7*, 623−628.
(36) Besenbacher, F. Scanning Tunnelling Microscopy Studies of Metal Surfaces. *Rep. Prog. Phys.* **1996**, *59*, 1737−1802.
(37) Laegsgaard, E.; österlund, L.; Thostrup, P.; Rasmussen, P. B.; Stensgaard, I.; Besenbacher, F. A High-Pressure Scanning Tunneling Microscope. *Rev. Sci. Instrum.* **2001**, *72*, 3537−3542.
(38) Kresse, G.; Hafner, J. Ab initiomolecular dynamics for open-shell transition metals. *Phys. Rev. B: Condens. Matter Mater. Phys.* **1993**, *48*, 13115−13118.
(39) Kresse, G.; Furthmüller, J. Efficient iterative schemes forab initiototal-energy calculations using a plane-wave basis set. *Phys. Rev. B: Condens. Matter Mater. Phys.* **1996**, *54*, 11169−11186.
(40) Blöchl, P. E. Projector Augmented-wave Method. *Phys. Rev. B: Condens. Matter Mater. Phys.* **1994**, *50*, 17953−17979.

DOI: 10.1021/acs.jpcc.9b09713
J. Phys. Chem. C 2019, 123, 30467−30472

(41) Kresse, G.; Joubert, D. From Ultrasoft Pseudopotentials to the Projector Augmented-wave Method. *Phys. Rev. B: Condens. Matter Mater. Phys.* **1999**, *59*, 1758−1775.
(42) Perdew, J. P.; Burke, K.; Ernzerhof, M. Generalized Gradient Approximation Made Simple. *Phys. Rev. Lett.* **1996**, *77*, 3865−3868.
(43) Grimme, S. Semiempirical GGA-type Density Functional Constructed with a Long-range Dispersion Correction. *J. Comput. Chem.* **2006**, *27*, 1787−1799.
(44) Tersoff, J.; Hamann, D. R. Theory of the Scanning Tunneling Microscope. *Phys. Rev. B: Condens. Matter Mater. Phys.* **1985**, *31*, 805−813.

DOI: 10.1021/acs.jpcc.9b09713
J. Phys. Chem. C 2019, 123, 30467−30472